PERGAMON

Atmospheric Environment 37 (2003) 1691–1701

ATMOSPHERIC ENVIRONMENT

www.elsevier.com/locate/atmosenv

Lagrangian stochastic modeling of a fluctuating plume in the convective boundary layer

Pasquale Franzese

School of Computational Sciences, George Mason University, MS 5C3, Fairfax, VA 22030, USA

Received 14 September 2002; accepted 12 December 2002

Abstract

A Lagrangian stochastic model of dispersion in the atmospheric convective boundary layer is derived. The turbulence is assumed to be non-homogeneous and non-Gaussian in the vertical direction, homogeneous and Gaussian in the horizontal directions. The model describes the evolution of an airborne contaminant in terms of motion of its centroid and diffusion of particles relative to the centroid. The vertical motion of the centroid is simulated using non-stationary Lagrangian stochastic equations incorporating a time-dependent filter for the turbulent energy. The filtering procedure removes the contribution of turbulent eddies smaller than the cloud instantaneous size to the meandering. The instantaneous dispersion of particles relative to the centroid is parameterized using inertial range similarity formulae. The model is applied to the case of continuous stationary releases and the crosswind dispersion is calculated according to Taylor's theory. The model satisfies the well-mixed condition and is capable of calculating all moments of concentration. Mean concentration and concentration fluctuations for several source heights are simulated and compared with laboratory observations.

Keywords: Concentration fluctuations; Air quality models; Particle models; Relative dispersion; Energy filter

1. Introduction

Gifford's (1959) analytical model proved to be a simple and effective tool for predicting concentration moments of order higher than the mean for stationary releases of contaminant in idealized homogeneous and Gaussian turbulence. The effects of internal concentration fluctuations, which were not accounted for in Gifford's original model, were effectively incorporated in that model by Yee and Wilson (2000) by assuming a functional form for the probability density function (pdf) of concentration relative to the plume centroid. Both Gifford (1959) and Yee and Wilson (2000) assume homogeneous turbulence and a Gaussian pdf of centroid positions in both the transverse and vertical directions.

To progress beyond this basic representation of the turbulence field, Luhar et al. (2000) proposed a Lagrangian stochastic model to calculate the pdf of plume centroid vertical position in the convective boundary layer (cbl), where the turbulence inhomogeneity along the vertical direction and the skewness of the turbulent vertical velocity determine a non-Gaussian vertical distribution of centroid positions and, ultimately, non-Gaussian concentration distributions of contaminant downwind of the source.

The trajectories of a plume or puff-centroid in a Lagrangian framework have been modeled in the past as simply equivalent to the trajectories of fluid particles (e.g., Yamada and Bunker, 1988; Weil, 1994). De Haan and Rotach (1998), using a different approach, calculate the centroid trajectories by first generating velocity time series of fluid particles using a Lagrangian stochastic model, then smoothing the calculated series using a filtering procedure, and finally integrating the smoothed velocities over time. Some difficulties in using the above approaches arise because the modeled centroid

E-mail address: pfranzes@gmu.edu (P. Franzese).

1352-2310/03/$ - see front matter
doi:10.1016/S1352-2310(03)00003-7

trajectories span the entire boundary layer height and hence the standard deviation of the centroid positions does not tend to zero in the far field. This behavior is unphysical, because the pdf of the centroid position in a bounded flow should reduce to a delta function when a well-mixed distribution of particles is reached. The model by Luhar et al. (2000) overcomes the theoretical difficulties inherent in the models mentioned above in that it ensures the correct partitions of particle position variance and third moment into meander and relative diffusion components, with the meander components vanishing in the far field. This model gives results in very good agreement with the observations.

The model presented in this paper is based on Gifford's (1959) meandering plume framework and on Luhar et al. (2000) idea of parameterizing the dispersion of the cloud relative to the centroid and using a Lagrangian stochastic model to calculate the pdf of vertical meander. The model predicts mean and all higher moments of the concentration field for continuous releases in a vertically inhomogeneous and skewed cbl flow.

The motion of the plume centroid is directly modeled using stochastic differential equations. However, while the motion of fluid particles is governed by the entire spectrum of turbulent kinetic energy, the motion of a cloud centroid is controlled only by the energy fluctuations with wavelengths larger than the cloud instantaneous characteristic scale. A simple formulation is presented, based on similarity theory relationships, for the partitioning of the turbulent energy into a component responsible for the centroid motion and a component responsible only for the generation of in-cloud velocity fluctuations, which are ineffective for the large scale motion of the bulk of the plume. The application of a time-dependent low-pass filter to the energy spectrum ensures that only the portion of energy governing the motion of the centroid is injected into the model at each instant in time. The centroid acceleration in the Lagrangian model is assumed to be a quadratic function of the centroid velocity and is determined according to the well-mixed condition (Thomson, 1987).

The complete model for the calculation of high-order concentration statistics is further developed using the assumption of homogeneous turbulence in the horizontal direction and a log-normal pdf of instantaneous concentration in a frame of reference relative to the centroid position.

The present model has the advantage of being simple and based on realistic assumptions. In addition, the filtering correction to the turbulent energy is suitable for straightforward applications to existing Lagrangian stochastic puff models because it uses the same framework of a standard one-particle model, that is, two stochastic differential equations driven by known turbulence statistics.

2. Basic equations for statistics of concentration

In this section, we summarize the equations defining the statistics of concentration in the fluctuating plume approach, where the pdf of concentration is described in terms of pdf of instantaneous concentration relative to the centroid location and pdf of centroid location.

By definition, the moments of concentration in a fixed coordinate system are written as

$$\overline{c^n}(x,y,z) = \int_0^\infty c^n p(c;x,y,z)\,\mathrm{d}c, \tag{1}$$

where c is the instantaneous concentration, p is the concentration pdf, x is the distance downwind of the source, y is the transverse coordinate with respect to the mean wind direction, z is the vertical coordinate with origin at ground level, and the bar indicates ensemble averaging. In the case of continuous release in stationary flow all ensemble averages coincide with time averages at any point in space (in the limit of infinite number of realizations and infinite averaging time). The fluctuating plume modeling approach is based on the following relationship for p (Gifford, 1959):

$$p(c;x,y,z) = \int\int p_{cr}(c|x,y,z,y_m,z_m) \times p_m(x,y_m,z_m)\,\mathrm{d}y_m\,\mathrm{d}z_m, \tag{2}$$

where $p_m(x,y_m,z_m)$ is the pdf of the location of the cloud instantaneous centroid (y_m,z_m) at x, and p_{cr} is the pdf of concentration relative to (y_m,z_m), i.e. in the frame of reference moving with the plume centroid, conditional on the centroid location. Since

$$\int_0^\infty c^n p_{cr}(c|x,y,z,y_m,z_m)\,\mathrm{d}c = \overline{c_r^n}(x,y,z,y_m,z_m), \tag{3}$$

where $\overline{c_r^n}$ are the concentration statistics at x relative to (y_m,z_m), it follows that

$$\overline{c^n}(x,y,z) = \int\int \overline{c_r^n} p_m(x,y_m,z_m)\,\mathrm{d}y_m\,\mathrm{d}z_m. \tag{4}$$

Eq. (4) states that the absolute concentration statistics $\overline{c^n}(x,y,z)$ can be calculated as the average of the relative concentration statistics $\overline{c_r^n}$ over the transverse and vertical trajectory of the plume centroid (y_m,z_m) at x. The plume meander along the transverse y-axis is assumed to be statistically independent of the meander along the vertical z-axis. Therefore, p_m can be decomposed as

$$p_m(x,y_m,z_m) = p_{ym}(x,y_m)p_{zm}(x,z_m). \tag{5}$$

In the following, we will develop a model to solve Eq. (4) with assumption (5).

3. Pdf of centroid location $p_m(x, y_m, z_m)$

In this section, we will determine p_m according to Eq. (5) by modeling separately p_{zm} and p_{ym}. A Lagrangian stochastic model will be developed to calculate p_{zm}, and a Gaussian pdf will be used to represent p_{ym}.

3.1. Pdf of centroid vertical location $p_{zm}(x, z_m)$

The pdf of centroid vertical location $p_{zm}(x, z_m)$ is calculated by simulating the vertical motion of the centroid, z_m, using a Lagrangian stochastic model and then sampling the simulated z_m at fixed points x.

The equations of motion of the centroid are written directly in the form of stochastic differential equations. The numerical solution to the equations of motion gives a statistical simulation of the centroid trajectories. Therefore, each realization corresponds to a possible snapshot of the plume centroid, and the ensemble average over many realizations gives the distribution of the plume centroid along x. The statistics of the centroid vertical velocity at fixed points x, i.e. the Eulerian statistics, are input into the equations of motion and need to be defined. Also, because the centroid vertical fluctuations decay with distance from the source, these Eulerian statistics depend on x.

3.1.1. Partition of energy

The motion of the centroid is controlled by the portion of the turbulent energy spectrum corresponding to wavelengths larger than the instantaneous cross-section scale of the plume. The residual portion of the spectrum includes the frequencies associated with smaller wavelengths and governs the dynamics within the cloud volume. The small energy wavelengths are responsible for the internal mixing and in-plume velocity fluctuations, which do not have a role in the bodily motion of the center of mass.

The vertical component of the turbulent kinetic energy σ_w^2 at any point in space can be partitioned as

$$\sigma_w^2 = \sigma_{wm}^2 + \sigma_{wr}^2, \tag{6}$$

where σ_{wm}^2 represents the fraction of energy responsible for the oscillating motion of the centroid and σ_{wr}^2 is the energy associated with the velocity fluctuations within the bulk of the cloud.

In homogeneous isotropic turbulence the following relationships can be written using simple similarity scaling: $\sigma_w^2 \propto (\varepsilon L)^{2/3}$ and $\sigma_{wr}^2 \propto (\varepsilon d)^{2/3}$, where ε is the dissipation rate of turbulent kinetic energy, L is the integral length scale of the turbulence, and d is a characteristic length scale of the cloud (Franzese and Borgas, 2002). While in the cbl the variation of σ_w^2 and σ_{wr}^2 along the vertical direction is significant, the variation of the *ratio* of σ_w^2 to σ_{wr}^2 is expected to be much smaller in that both these functions are affected in a similar way by the vertical inhomogeneities of the heat flux and ε. Therefore, in the cbl we can write to a first approximation $\sigma_w^2 = (\varepsilon H)^{2/3} f(z)$ and $\sigma_{wr}^2 = (\varepsilon d)^{2/3} f(z)$, where H is the mixed layer depth which we assume to be proportional to L, and f is a non-dimensional function. Note that, because by virtue of the scaling properties of the cbl we can write $\varepsilon = (w_*^3/H) g(z)$, where w_* is the convective velocity scale and g is a non-dimensional function, the above expression for σ_w^2 can also be written as $\sigma_w^2 = w_*^2 h(z)$, where $h = f g^{2/3}$, which is the form that is commonly used to parameterize σ_w^2 in the cbl [see, e.g., Eq. (16)]. The simple formula below follows immediately from Eq. (6)

$$\sigma_{wm}^2 = \sigma_w^2 \left[1 - \left(\frac{d}{H} \right)^{2/3} \right]. \tag{7}$$

Eq. (7) relates the energy of the fluctuations of the cloud centroid σ_{wm}^2 to the turbulent energy σ_w^2. Since the size of the cloud, d, is a function of time, the term $1 - (d/H)^{2/3}$ is in fact a time-dependent low-pass filter: for a source size $\sigma_0 \ll H$, σ_{wm}^2 is approximately equal to σ_w^2 at the source, when almost all turbulent energy contributes to the bulk motion, and tends to zero at large distances, as d tends to the turbulence length scale H and fewer and fewer energy wavelengths actively feed the meandering process. Conversely, the internal fluctuation energy component σ_{wr}^2 is very small near the source, but it equals the total turbulent energy in the far field, where the vertical meander fades out as the plume distributes uniformly along the boundary layer height (by definition, the in-plume velocity fluctuations in a well-mixed plume coincide with the turbulent velocity fluctuations).

The characteristic size of the bulk of the plume, d, is related to the vertical component of the separation vector between any two particles of the cloud. We assume that the turbulence which governs the relative diffusion process can be treated as locally homogeneous by averaging two-point velocity statistics and energy dissipation rate over the domain of interest (Franzese and Borgas, 2002; Luhar et al., 2000). A simple and robust parameterization of d is obtained using the inertial range formulation for the two-particle relative separation, which we write as

$$\overline{r^2} = C_r \varepsilon (t_s + t)^3, \tag{8}$$

where r is the magnitude of the separation vector between any two particles of the cloud, $t_s = [\sigma_0^2/(C_r \varepsilon)]^{1/3}$ accounts for a finite initial source size σ_0, and C_r is the Richardson–Obukhov constant. Eq. (8) can be obtained directly from the Richardson–Obukhov 4/3 law and fits well the simulation data points reported in Franzese and

Borgas (2002), although it is slightly inaccurate at very short time as it does not account for the effects of the initial separation velocity, which give $\overline{r^2} \propto t^2$ up to $t \sim (\sigma_0^2/\varepsilon)^{1/3}$ (Batchelor, 1952). The constant C_r was assumed to be 1.4 based on the values of the relative vertical spread σ_{zr} observed in the water tank experiments of dispersion in the cbl by Hibberd (2000) (reported in Fig. 3a below). The average effective size of the plume bulk d was determined assuming that the plume is perfectly well mixed after a non-dimensional travel time $T = (t + t_s)w_*/H = 6$. Because for a well-mixed plume σ_{wm} vanishes and $d = H$, we obtain $d \approx (\overline{r_1^2})^{1/2}/6.3$, where r_1 is a component of the separation vector (i.e., $\overline{r_1^2} = \overline{r^2}/3$).

3.1.2. Lagrangian model for cloud centroid trajectories

We assume that independent realizations of the motion of a cloud centroid in the vertical direction z can be described by the following stochastic differential equations:

$$\begin{aligned} \mathrm{d}w_m(t) &= a_m(t, w_m, z_m)\,\mathrm{d}t + b(t, z_m)\,\mathrm{d}W, \\ \mathrm{d}z_m(t) &= w_m(t)\,\mathrm{d}t, \end{aligned} \tag{9}$$

where w_m is the vertical velocity of the centroid, a_m is a deterministic acceleration term, b is a time- and height-dependent coefficient, and $\mathrm{d}W$ are the increments of a Wiener process with zero mean and variance $\mathrm{d}t$. Eqs. (9) are based on the assumption that the joint evolution of position and velocity of the centroid can be represented by a Markov process, that is commonly used in one-particle Lagrangian stochastic models (Thomson, 1987). In our case the same assumption holds because the motion of the centroid is still governed by turbulent velocity fluctuations (as is the motion of a fluid particle), although the fluctuation frequencies include only a subset of the entire energy spectrum. The coefficient of the random term, b, is written as $b = (2\sigma_{wm}^2/T_{zm})^{1/2}$ where T_{zm} is the time-dependent Lagrangian decorrelation time scale of the vertical meander. T_{zm} can be defined as the ratio of centroid vertical spread to standard deviation of the centroid vertical velocity, and hence be written as

$$T_{zm} = \sqrt{\frac{H^2 - d^2}{\sigma_{wm}^2}}. \tag{10}$$

The drift term $a_m(t, w_m, z_m)$ will be derived from the Fokker–Planck equation associated with Eqs. (9) that describes the evolution of $P_{Lm}(t, w_m, z_m|t_0, w_{m0}, z_{m0})$, i.e. the Lagrangian pdf of w_m at a given height z_m at time t, given the initial conditions indicated by the subscript "0". Because $\int P_{Lm}\,\mathrm{d}t_0\,\mathrm{d}w_{m0}\,\mathrm{d}z_{m0} = P_{Em}(t, w_m|z_m)$, where P_{Em} is the Eulerian pdf of w_m at fixed points z_m, and where the integration is taken over the domain of definition of the set of initial conditions (t_0, w_{m0}, z_{m0}), the Fokker–Planck equation for P_{Lm} integrated over t_0, w_{m0}, and z_{m0} becomes

$$\frac{\partial P_{Em}}{\partial t} + w_m \frac{\partial P_{Em}}{\partial z_m} = -\frac{\partial a_m P_{Em}}{\partial w_m} + \frac{b^2}{2}\frac{\partial^2 P_{Em}}{\partial w_m^2}. \tag{11}$$

Eq. (11) establishes a relationship between the Eulerian statistics of w_m at fixed downwind distances x and heights z_m and the centroid equations of motion (9). Therefore, it ensures the fulfillment of the well-mixed condition (Thomson, 1987) applied to the motion of the centroid. We assume that the acceleration is a functional form of the velocity as follows:

$$a_m(t, w_m, z_m) = \alpha(t, z_m)w_m^2 + \beta(t, z_m)w_m + \gamma(t, z_m), \tag{12}$$

where the three unknown coefficients α, β and γ are determined by multiplying Eq. (11) successively by powers of w_m, and then integrating over w_m. A similar type of quadratic form closure was used by Franzese et al. (1999) in the context of a one-particle model in the cbl. One obtains

$$\begin{aligned} \alpha = {} & \frac{(\partial_t \overline{w_m^3} + \partial_{zm}\overline{w_m^4})/3}{\overline{w_m^4} - \overline{w_m^3}^2/\sigma_{wm}^2 - \sigma_{wm}^4} \\ & - \frac{\overline{w_m^3}(\partial_t \sigma_{wm}^2 + \partial_{zm}\overline{w_m^3} - 2\sigma_{wm}^2/T_{zm})/(2\sigma_{wm}^2) - \sigma_{wm}^2 \partial_{zm}\sigma_{wm}^2}{\overline{w_m^4} - \overline{w_m^3}^2/\sigma_{wm}^2 - \sigma_{wm}^4}, \end{aligned} \tag{13}$$

$$\beta = \frac{\partial_t \sigma_{wm}^2 + \partial_{zm}\overline{w_m^3} - 2\alpha\overline{w_m^3}}{2\sigma_{wm}^2} - \frac{1}{T_{zm}}, \tag{14}$$

$$\gamma = \partial_{zm}\sigma_{wm}^2 - \alpha\sigma_{wm}^2, \tag{15}$$

where ∂ denotes differentiation with respect to its subscript variable.

σ_{wm}^2 is given by Eq. (7); $\overline{w_m^3}$ and $\overline{w_m^4}$ are determined according to Eq. (7) assuming that the pdf of w_m has the same skewness and kurtosis factors as the pdf of w, that is, $\overline{w_m^3} = \overline{w^3}[1 - (d/H)^{2/3}]^{3/2}$ and $\overline{w_m^4} = \overline{w^4}[1 - (d/H)^{2/3}]^2$. The analytical expressions for the vertical profiles of σ_w^2 and $\overline{w^3}$ are taken to be the same as those used by Luhar et al. (2000)

$$\sigma_w^2 = w_*^2 a_1 \left[\frac{z}{H}\left(1 - a_2\frac{z}{H}\right)\left(1 - \frac{z}{H}\right)\right]^{2/3}, \tag{16}$$

$$\overline{w^3} = w_*^3 a_3 \frac{z}{H}\left(1 - \frac{z}{H}\right)^{3/2}, \tag{17}$$

where the coefficients a_1, a_2 and a_3 were estimated by least-squares fits to several sets of experimental data reported by Franzese et al. (1999) and are equal to 1.7, 0.7 and 1.2, respectively. The kurtosis factor of the vertical velocity distribution is taken equal to 3.5, i.e. $\overline{w^4} = 3.5\sigma_w^4$.

Because for relatively small sources the distribution of w_m at the source is approximately equal to the Eulerian turbulent vertical velocity pdf at the source height z_s, $P_E(w|z_s)$, the initial velocities w_m for each realization in Eq. (9) were chosen by sampling $P_E(w|z_s)$ as described in

Luhar and Britter (1989). Each simulation consists of 20,000 realizations with an adaptive time step $dt = 0.001T_{zm}$. Perfect reflection at the boundaries was assumed whenever the distance between the centroid and one of the boundaries was smaller than the characteristic radius of the plume bulk $d/2$.

3.2. Pdf of centroid transverse location $p_{ym}(x, y_m)$

Because the turbulence is assumed to be homogeneous in the horizontal directions, the transverse distribution of centroid positions is Gaussian (Gifford, 1959; Yee and Wilson, 2000):

$$p_{ym}(x, y_m) = \frac{1}{\sqrt{2\pi}\sigma_{ym}} \exp\left(-\frac{y_m^2}{2\sigma_{ym}^2}\right), \tag{18}$$

where the centroid transverse dispersion coefficient σ_{ym} is calculated as $\sigma_{ym}^2 = \sigma_y^2 - \sigma_{yr}^2$, with the crosswind spread σ_y^2 given by Taylor's formula: $\sigma_y^2 = 2\sigma_v^2 T_{Lv}\{t - T_{Lv}[1 - \exp(-t/T_{Lv})]\}$. The transverse Lagrangian time scale is calculated as $T_{Lv} = 2\sigma_v^2/(C_0\varepsilon)$, with the constant $C_0 = 3$, the turbulence transverse velocity variance $\sigma_v^2 = 0.2w_*^2$ and $\varepsilon = 0.4w_*^3/H$. The value of C_0 was chosen to fit the observations of σ_y in the laboratory experiments of Willis and Deardorff (1976, 1978, 1981) and the LES results of Nieuwstadt (1992); the parameterizations of σ_v and ε are the same as those used by Luhar et al. (2000). The value of σ_v was based on the LES and laboratory data reported by Hibberd and Sawford (1994), ε was based on LES and field data as described in Luhar et al. (1996). The transverse relative dispersion coefficient σ_{yr} was parameterized as

$$\sigma_{yr}^2 = \frac{C_{yr}\varepsilon(t_s + t)^3}{\{1 + [C_{yr}\varepsilon t^2/(2\sigma_v^2 T_{Lv})]^{2/3}\}^{3/2}}, \tag{19}$$

where $C_{yr} = C_r/6$. Eq. (19) corresponds to the inertial range relative dispersion formulation $\sigma_{yr}^2 = C_{yr}\varepsilon(t_s + t)^3$ at small time, and tends to Taylor's limit $\sigma_{yr}^2 = 2\sigma_v^2 T_{Lv} t$ at large time. Both σ_{ym} and σ_{yr} are in good agreement with the LES results of Nieuwstadt (1992) (not reproduced here).

4. Mean concentration

In this section, we determine the mean relative concentration $\bar{c}_r$ and calculate the mean concentration field $\bar{c}$ according to Eq. (4). Then, we present some simulation results along with the corresponding laboratory datasets. The results include plots of crosswind-integrated mean concentration contours, mean particle height, vertical spread, relative vertical spread, and centroid vertical spread. All of the simulations were run for three source heights, for which laboratory data were available.

4.1. Mean relative concentration $\bar{c}_r$

The instantaneous ensemble mean concentration relative to the cloud center of mass at a given downwind distance x is defined as

$$\bar{c}_r = (Q/\bar{u})p_{yr}(x, y, y_m)p_{zr}(x, z, z_m), \tag{20}$$

where Q is the amount of material released per unit time, $\bar{u}$ is the mean cloud advection velocity which we assume to be constant throughout the boundary layer height, and p_{yr} and p_{zr} are the transverse and vertical pdfs of mean particle positions relative to the centroid, respectively. We assume that the particle mean distribution around the center of mass is Gaussian in both the transverse and the vertical directions

$$p_{yr}(x, y, y_m) = \frac{1}{\sqrt{2\pi}\sigma_{yr}} \exp\left[-\frac{(y - y_m)^2}{2\sigma_{yr}^2}\right], \tag{21}$$

$$p_{zr}(x, z, z_m) = \frac{1}{\sqrt{2\pi}\tilde{\sigma}_{zr}} \sum_{n=-N}^{N} \left\{\exp\left[-\frac{(z - z_m + 2nH)^2}{2\tilde{\sigma}_{zr}^2}\right] + \exp\left[-\frac{(z + z_m + 2nH)^2}{2\tilde{\sigma}_{zr}^2}\right]\right\}, \tag{22}$$

where N was taken equal to 10 and the relative vertical dispersion coefficient $\tilde{\sigma}_{zr}$ was parameterized as

$$\tilde{\sigma}_{zr}^2(t) = \frac{C_{zr}\varepsilon(t_s + t)^3}{[1 + (C_{zr}\varepsilon t^3/0.16)^{2/3}]^{3/2}}, \tag{23}$$

where $C_{zr} = C_r/6$. Eq. (23) is consistent with the inertial range form (8) at small time, and accounts for the effect of the boundaries that reduce the rate of relative vertical spread as t increases. Because Eq. (22) includes multiple reflections at the boundaries, the coefficient $\tilde{\sigma}_{zr}^2$ does not represent the effective relative vertical dispersion variance σ_{zr}^2, which is given by $\int\int(z - z_m)^2 p_{zr}p_{zm}\,dz\,dz_m$. The numerical coefficient and the powers in the denominator of Eq. (23) have been selected so that σ_{zr} and the centroid vertical spread σ_{zm} fit the corresponding laboratory data of Hibberd (2000) up to a time t_1 of about $6H/w_*$, where σ_{zr} is only about 0.1% smaller than its equilibrium value. At times larger than t_1 a virtually perfect uniform spread can be reached by using a formula of the type $\tilde{\sigma}_{zr}^2(t) = \tilde{\sigma}_{zr}^2(t_1) + (d\tilde{\sigma}_{zr}^2/dt)_{t_1}(t - t_1)$ in Eq. (22).

Because of the Gaussian form of p_{zr}, the distribution of $\bar{c}_r$ does not include additional skewness in the vertical direction beyond that caused by the reflections at the boundaries. Therefore, $\overline{z^3}$ is not partitioned into a meander component $\overline{z_m^3}$ and a relative diffusion component $\overline{(z - z_m)^3}$, and $\overline{c^3}$ is entirely due to the skewness of p_{zm} and to boundary reflections. This approximation was not found to introduce a significant error in the simulated concentration field, possibly because $\overline{(z - z_m)^3}$ is relatively small in the near field, due to the small size

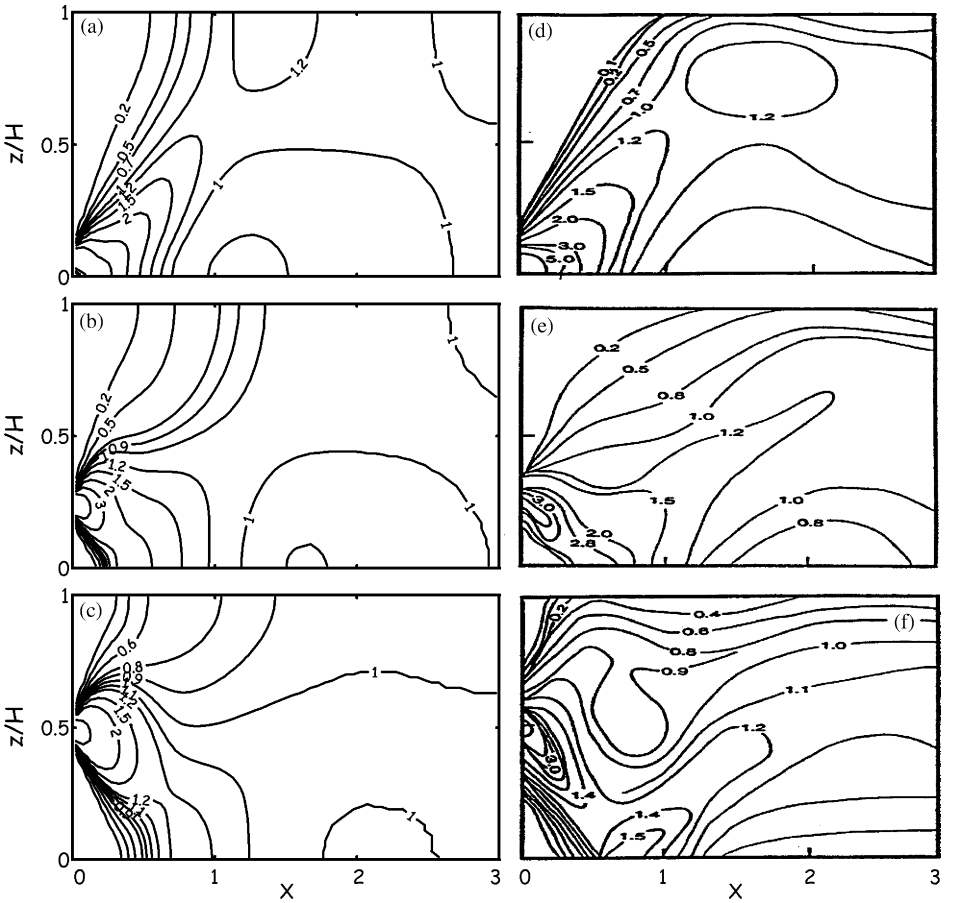

Fig. 1. Non-dimensional crosswind-integrated mean concentration contours predicted by the model (left) and observed in the water tank experiments by Willis and Deardorff (1976, 1978, 1981) (right) for the source heights $z_s = 0.067H$ (top), $0.24H$ (center) and $0.49H$ (bottom).

of the plume, and tends to zero in the far field as the plume tends to be well mixed.

4.2. Mean concentration results

The mean concentration field can be now calculated according to Eq. (4), which we write in the more convenient form below after integrating over the centroid transverse coordinate y_m:

$$\bar{c}(x,y,z) = \frac{Q}{\sqrt{2\pi}\bar{u}\sigma_y}\exp\left(-\frac{y^2}{2\sigma_y^2}\right) \times \int_0^H p_{zr}(x,z,z_m)p_{zm}(x,z_m)\,\mathrm{d}z_m, \quad (24)$$

where p_{zr} is the analytical Gaussian distribution (22), and p_{zm} is calculated using our Lagrangian stochastic model (9). To test mean concentration distribution results, dispersion simulations were performed for three source heights, for which data are available from the water tank experiments of Willis and Deardorff (1976, 1978, 1981). The trajectory of the centroids was followed until a travel time $t = 3H/w_*$, corresponding to a non-dimensional downwind distance $X = xw_*/(\bar{u}H) = 3$. Figs. 1a–c present the contour plots of the non-dimensional crosswind-integrated mean concentration obtained from our model for the source heights $z_s = 0.067H$, $0.24H$ and $0.49H$, respectively. The dimensions of the cells are $\Delta X = 0.05$ and $\Delta(z/H) = 0.02$. The corresponding contour plots obtained by Willis and Deardorff (1976, 1978, 1981) are shown in Figs. 1d–f.

The model results show good overall agreement with the laboratory data and accurately reproduces the characteristics of the mean concentration field in the cbl. For instance, Fig. 1a ($z_s = 0.067H$) shows the ascent of the maximum concentration above z_s up to a maximum height of about $0.8H$ and its subsequent slight descent; Figs. 1b and c ($z_s = 0.24H$ and $z_s = 0.49H$, respectively) show the initial descent of the

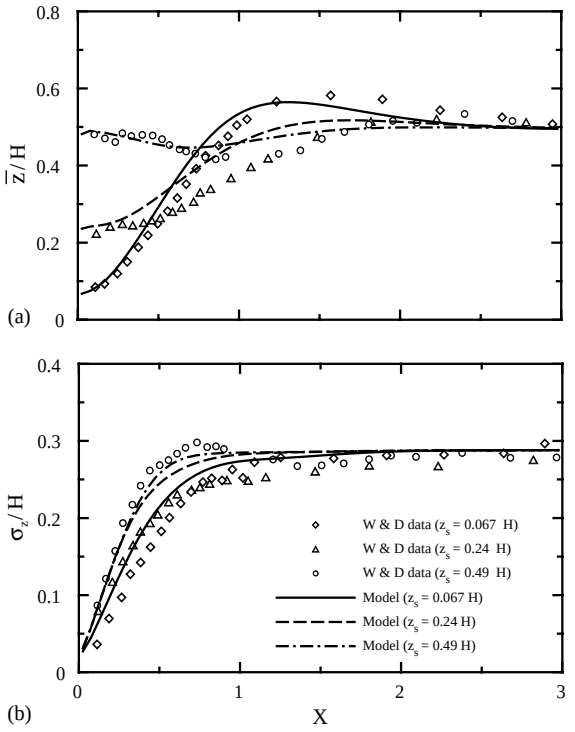

Fig. 2. Non-dimensional mean particle height (a) and vertical spread (b) predicted by the model, along with the data from the water tank experiments of Willis and Deardorff (1976, 1978, 1981, referred to in the figure as W & D) for the source heights $z_s = 0.067H$, $0.24H$ and $0.49H$.

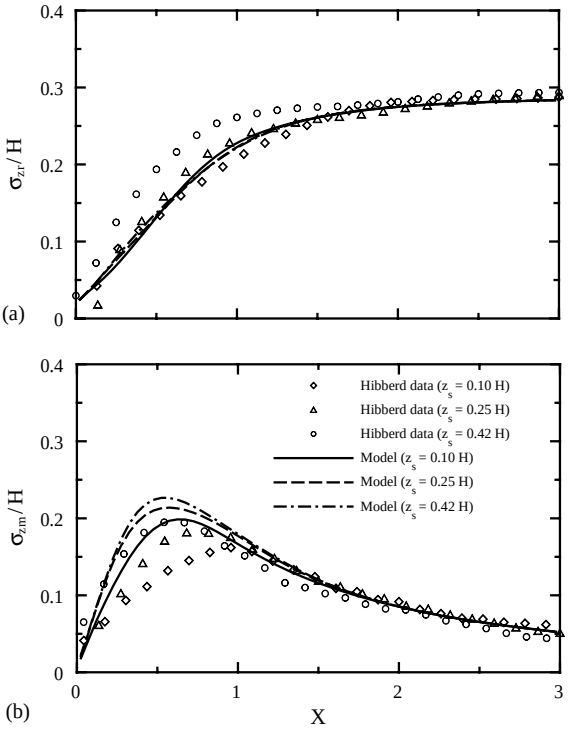

Fig. 3. Non-dimensional relative vertical spread σ_{zr}/H (a) and centroid vertical spread σ_{zm}/H (b), along with the water tank data of Hibberd (2000) for the source heights $z_s = 0.10H$, $0.25H$ and $0.42H$.

maximum concentration to the ground followed by an ascent farther downwind.

The model-simulated non-dimensional mean particle height $\bar{z}/H$ and vertical spread σ_z/H are plotted in Figs. 2a and b, respectively, along with the data reported by Willis and Deardorff (1976, 1978, 1981). The model compares well with the data although for the source height at $0.24H$, at small distance ($X < 1.5$), it overpredicts the experimentally observed $\bar{z}$ and σ_z by 10–15%. Overpredictions of the same order are observed in analogous simulations by one-particle stochastic models (e.g. Franzese et al., 1999; Luhar et al., 2000) and may depend on the selected vertical profiles of turbulence statistics and energy dissipation rate.

Fig. 3a shows three simulations of the non-dimensional relative vertical spread σ_{zr}/H for $z_s = 0.10H$, $0.25H$ and $0.42H$, respectively, where σ_{zr} was calculated at each x as the square root of $\sigma_{zr}^2 = \int\int (z - z_m)^2 p_{zr} p_{zm}\, dz\, dz_m$. The saline water tank data of Hibberd (2000) are also shown. The model σ_{zr} is in good agreement with the data, although it shows a dependence on the source height weaker than the observations. This is possibly due to the simple parameterization (23) for $\tilde{\sigma}_{zr}$, which is independent of z.

Fig. 3b shows the non-dimensional vertical spread of the plume centroid σ_{zm}/H, where σ_{zm} was calculated as $(\sigma_z^2 - \sigma_{zr}^2)^{1/2}$, along with the data of Hibberd (2000). The model predicts larger peak values for higher sources in agreement with the observed pattern, although it slightly overpredicts the maxima. The model curves fit the data with a minimal error at all $X > 1$.

5. Concentration fluctuations and higher order statistics of concentration

In this section, we determine the expression for the moments of c. We parameterize p_{cr} using an analytical pdf and give the formula for the moments of relative concentration $\overline{c_r^n}$, which are necessary to calculate $\overline{c^n}$ according to Eq. (4). We perform a simulation of the concentration fluctuation intensity field $i_c = \sigma_c/\bar{c}$, where σ_c is the standard deviation of concentration, and compare the crosswind averages of i_c over inner and outer regions of the plume at several downwind distances with the corresponding laboratory observations.

5.1. Pdf of relative concentration p_{cr} and moments of concentration

The pdf of relative concentration p_{cr}, which represents the instantaneous distribution of material around the plume centroid, is parameterized using a log-normal pdf. Csanady (1973) obtained a log-normal distribution of relative concentration as the result of a model that described the mixing process within a contaminant cloud. According to Csanady's (1973) model, each parcel of the cloud is assumed to change its concentration through a succession of diluting impulses: in each impulse the parcel is mixed with a random portion of uncontaminated fluid. It is possible to choose other forms for this distribution, for example Hanna (1984) used an exponential pdf, and Yee and Wilson (2000) and Luhar et al. (2000) used a gamma pdf which proved to describe the internal structure of a plume with good accuracy. After testing our model using a gamma pdf as p_{cr}, we did not find any significant discrepancy with the results obtained using the algebraically simpler log-normal pdf, which was therefore selected. The log-normal distribution is written as

$$p_{cr}(c|x,y,z,y_m,z_m) = \frac{1}{\sqrt{2\pi}sc}\exp\left[-\frac{(\ln c-\mu)^2}{2s^2}\right], \qquad (25)$$

where $s=\sqrt{\ln(1+i_{cr}^2)}$, and $\mu=\ln(\bar{c}_r/\sqrt{1+i_{cr}^2})$; $i_{cr}=\sigma_{cr}/\bar{c}_r$ denotes the intensity of relative concentration fluctuations, where σ_{cr} is the standard deviation of relative concentration. The moments of c_r calculated using Eq. (25) assume the simple form below

$$\overline{c_r^n}=\bar{c}_r^n(1+i_{cr}^2)^{n(n-1)/2}. \qquad (26)$$

To date there are no available observations of i_{cr} in the cbl. Luhar et al. (2000) set an iterative procedure to determine the values of i_{cr} that produce the best fit of their simulated intensity of absolute concentration $i_c=\sigma_c/\bar{c}$ to laboratory data. We parameterized i_{cr} by least-squares fitting the curve reported in Luhar et al. (2000) as follows:

$$i_{cr}=b_1X^3\exp(-X^{2/3}/b_2), \qquad (27)$$

where $b_1=60$ and $b_2=0.27$.

All moments of $c(x,y,z)$ can be now calculated according to Eq. (4), which can be written in the following form after integrating over y_m:

$$\overline{c^n}(x,y,z)=\frac{Q}{\bar{u}}\left[\frac{(1+i_{cr}^2)^{n-1}}{2\pi\sigma_{yr}^2}\right]^{n/2}\left(\frac{\sigma_{yr}^2}{n\sigma_{ym}^2+\sigma_{yr}^2}\right)^{1/2}\times\exp\left[-\frac{ny^2}{2(n\sigma_{ym}^2+\sigma_{yr}^2)}\right]\times\int_0^H p_{zr}^n(x,z,z_m)p_{zm}(x,z_m)\,\mathrm{d}z_m. \qquad (28)$$

Obviously, for $n=1$ this equation coincides with Eq. (24) for $\bar{c}$.

5.2. Concentration fluctuations results

Deardorff and Willis (1984) report water tank observations of near-surface concentration fluctuation intensity $i_c=\sigma_c/\bar{c}$. The experiments were conducted for a source size $\sigma_0=0.003H$ at a height of $0.13H$. Because the laboratory plume had a non-zero initial momentum, a virtual source height $z_s=0.22H$ was assumed in our simulations, as estimated by Luhar et al. (2000).

Contours of the calculated i_c at the plume centerplane $y=0$ are shown in Fig. 4 for the above input conditions. The vertical profiles of i_c in Fig. 4 consistently show larger values at the boundaries than within the boundary layer, with the lowest values located near the plume centroid. At distances X larger than about 6, the vertical variations of i_c are not appreciable. An interesting feature of the computed field in Fig. 4 is the occurrence of a ground-level local minimum of $i_c\approx1.4$ at $X\approx0.4$, and of a local maximum of about 2 at $X\approx1.2$. These points are the result of a balance between two effects. On the one hand, the intensity of fluctuations along the plume mean trajectory decays with X after an initial stage of growth because the vertical spread is constrained by the boundaries; on the other hand, at a fixed X, i_c always increases with distance from the centroid. Therefore, the ascent of the plume at $0.5<X<1.5$ causes the ground level i_c in that region to increase with X at a rate higher than the decay rate, thus forming a local maximum.

The existence of the predicted local maximum and minimum is supported by Deardorff and Willis' (1984) experimental data. Fig. 5 presents the observed and predicted i_c as a function of X at a height $z=0.08H$. Only the data from the experiments with non-buoyant emissions are considered here. The observed values of i_c

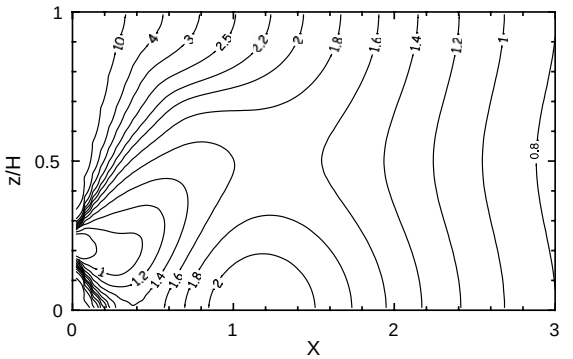

Fig. 4. Contours of the concentration fluctuation intensity i_c along the plume centerplane $y=0$ predicted by the model for a source with size $\sigma_0=0.003H$ at a height $z_s=0.22H$.

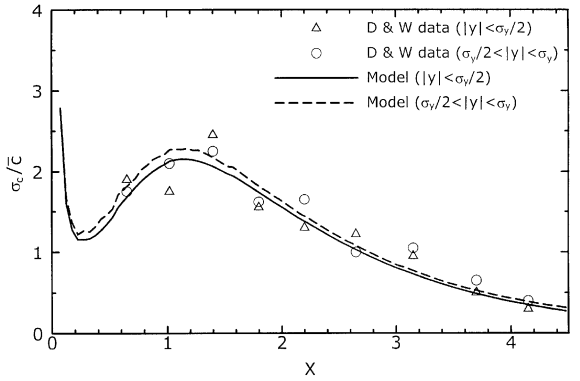

Fig. 5. Concentration fluctuation intensity i_c as a function of the non-dimensional distance X at a height $z = 0.08H$ for a source with size $\sigma_0 = 0.003H$ at a height $z_s = 0.22H$. The observations from the water tank experiments by Deardorff and Willis (1984, referred to in the figure as D & W) averaged over $|y|<\sigma_y/2$ are represented by open triangles, over $\sigma_y/2<|y|<\sigma_y$ by open circles. The corresponding predicted i_c are represented by the solid and the dashed line, respectively.

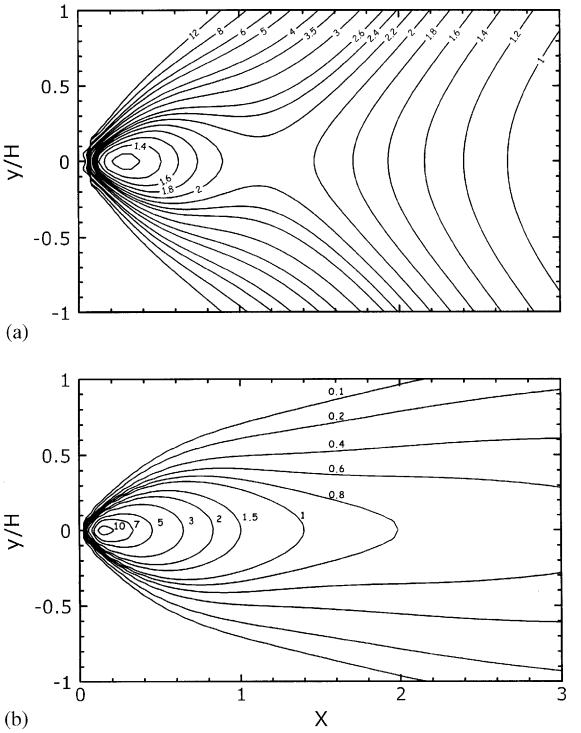

Fig. 6. Contours of concentration fluctuation intensity i_c (a) and of non-dimensional mean concentration $\bar{c}\,\bar{u}H^2/Q$ (b) at $z = 0.08H$ predicted by the model for a source with size $\sigma_0 = 0.003H$ at a height $z_s = 0.22H$.

averaged over $|y|<\sigma_y/2$ are represented by open triangles, those averaged over $\sigma_y/2<|y|<\sigma_y$ by open circles. The lines correspond to the predicted i_c averaged over its values at $|y| = 0$, $\sigma_y/4$ and $\sigma_y/2$ (solid line), and over $|y| = \sigma_y/2$, $3\sigma_y/4$ and σ_y (dashed line). The model results are in good agreement with the observations, including the prediction of a peak followed by a monotonic decay with distance in both the inner and the outer region. Deardorff and Willis (1984) caution about the validity of the high values observed at $X \approx 1.4$, arguing that these data might be anomalous due to the low number of realizations which were used to form the ensemble means. In fact, the existence of a peak of i_c has been confirmed by our model results in Fig. 5, and has been simply explained by analyzing the fluctuation intensity contours in Fig. 4.

Additional detail is provided by the near-surface ($z = 0.08H$) fluctuation intensity field, which is depicted in Fig. 6a. This figure shows that a local minimum and maximum of i_c are formed downwind of the source only at $|y|<H/4$ approximately. At transverse distances beyond $|y| \approx H/4$, i_c simply decreases with X for all $X > 0$. The corresponding near-surface non-dimensional mean concentration field $\bar{c}\,\bar{u}H^2/Q$ at $z = 0.08H$ is presented in Fig. 6b. The maximum concentration occurs at $X \approx 0.3$ and has a magnitude of about 10. Note that while the minimum near-surface i_c at $X \approx 0.5$ (Fig. 6a) occurs near the location of maximum $\bar{c}$ (Fig. 6b), it is not possible to predict the existence of the near-surface local maximum i_c at $X \approx 1.2$ simply on the basis of the mean concentration field in Fig. 6b.

6. Conclusions

The present form of the model has been derived prioritizing simplicity and robustness. For instance, basic parameterizations of two-particle relative dispersion and particle mean vertical distribution around the centroid have been used [Eqs. (8) and (22), respectively], and a log-normal pdf has been preferred to the more complex gamma pdf to represent the relative concentration distribution [Eq. (25)]. In some cases it is possible to use more detailed parameterizations, but the overall good accordance of the model results with observations suggests that the present formulation already ensures the level of accuracy required in most applications.

The Lagrangian model responds to the need of well-founded particle models where mass kernels are associated to the released particles. In such a representation, the dynamics of mass centroids cannot be equated with the dynamics of single particles because they correspond to different physical processes. The proposed filtering technique is simple and can be separately incorporated in other existing Lagrangian formulations of one-particle models for mean concentration fields with relatively small effort.

The centroid acceleration has been approximated by a quadratic function of the centroid velocity and has been determined in terms of filtered turbulent velocity statistics. This type of functional form closure was used to determine particle accelerations in the context of one-particle models, where it proved to produce accurate mean concentration fields with a good computational efficiency due to its simplicity (e.g., Franzese et al., 1999; Öttl et al., 2001). This approach avoids the need to assume an analytical form for the pdf of the turbulent velocity and allows directly the use of the observed turbulence velocity statistics up to the fourth order. Moreover, it does not require preliminary generation of Lagrangian one-particle dispersion statistics. Because the plume size increases with time, the filtered centroid velocity statistics are functions of time, hence the acceleration is time-dependent and the equations of motion for the centroid are non-stationary. This is a natural mathematical framework to describe the centroid damped oscillations, which fade out as the contaminant cloud distributes uniformly along the vertical direction.

The agreement between the dispersion results obtained from the new model and the available laboratory data is very good. Furthermore, the simulations clearly show a non-monotonic decay of the near-surface intensity of concentration fluctuations. We elucidated the mechanisms responsible for the occurrence of a local minimum and maximum intensity of fluctuation, and showed how this phenomenon is consistent with the mean concentration patterns. This peculiar behavior is in accordance with the laboratory experiments of Deardorff and Willis (1984), where the observations of a local maximum could not be explained were attributed to a possible statistical uncertainty.

The model for the calculation of second and higher order concentration statistics uses the intensity of relative concentration fluctuations i_{cr} as input. The parameterization of i_{cr} was based on the data that Luhar et al. (2000) determined using an iterative procedure. Although the good agreements of both Luhar et al. (2000) and the present model results with observations suggest that the parameterized i_{cr} is realistic, it is hoped that experimental estimations of this quantity could substantiate, if not improve, its current definition.

Acknowledgements

This research was sponsored by the US Defense Threat Reduction Agency (DTRA), with Major Brian A. Beitler as technical contract representative. The writer would like to thank Mark Hibberd for kindly providing his laboratory data.

References

Batchelor, G.K., 1952. Diffusion in a field of homogeneous turbulence. II. The relative motion of particles. Proceedings of the Cambridge Philosophical Society 48, 345–362.

Csanady, G.T., 1973. Turbulent Diffusion in the Environment. D. Reidel Publishing Company, Dordrecht, Holland, p. 228.

Deardorff, J.W., Willis, G.E., 1984. Groundlevel concentration fluctuations from a buoyant and a non-buoyant source within a laboratory convectively mixed layer. Atmospheric Environment 18, 1297–1309.

De Haan, P., Rotach, M.W., 1998. A novel approach to atmospheric dispersion modelling: the Puff-Particle Model (PPM). Quarterly Journal of the Royal Meteorological Society 124, 2771–2792.

Franzese, P., Borgas, M.S., 2002. A simple relative dispersion model for concentration fluctuations in clouds of contaminant. Journal of Applied Meteorology 41, 1101–1111.

Franzese, P., Luhar, A.K., Borgas, M.S., 1999. An efficient Lagrangian stochastic model of vertical dispersion in the convective boundary layer. Atmospheric Environment 33, 2337–2345.

Gifford, F.A., 1959. Statistical properties of a fluctuating plume dispersion model. Advances in Geophysics 6, 117–137.

Hanna, S.R., 1984. Concentration fluctuations in a smoke plume. Atmospheric Environment 18, 1091–1106.

Hibberd, M.F., 2000. Vertical dispersion of a passive scalar in the convective boundary layer: new laboratory results. Preprints of 11th AMS Conference on the Applications of Air Pollution Meteorology, American Meteorological Society, Boston, pp. 18–23.

Hibberd, M.F., Sawford, B.L., 1994. A saline laboratory model of the planetary convective boundary layer. Boundary-Layer Meteorology 67, 229–250.

Luhar, A.K., Britter, R.E., 1989. A random walk model for dispersion in inhomogeneous turbulence in a convective boundary layer. Atmospheric Environment 23, 1911–1924.

Luhar, A.K., Hibberd, M.F., Hurley, P.J., 1996. Comparison of closure schemes used to specify the velocity PDF in Lagrangian Stochastic dispersion models for convective conditions. Atmospheric Environment 30, 1407–1418.

Luhar, A.K., Hibberd, M.F., Borgas, M.S., 2000. A skewed meandering-plume model for concentration statistics in the convective boundary layer. Atmospheric Environment 34, 3599–3616.

Nieuwstadt, F.T.M., 1992. A large-eddy simulation of a line source in a convective atmospheric boundary layer—I. Dispersion characteristics. Atmospheric Environment 26A, 485–495.

Öttl, D., Almbauer, R.A., Sturm, P.J., 2001. A new method to estimate diffusion in stable, low wind conditions. Journal of Applied Meteorology 40, 259–268.

Thomson, D.J., 1987. Criteria for the selection of stochastic models of particle trajectories in turbulent flows. Journal of Fluid Mechanics 180, 529–556.

Weil, J.C., 1994. A hybrid Lagrangian dispersion model for elevated sources in the convective boundary layer. Atmospheric Environment 28, 3433–3448.

Willis, G.E., Deardorff, J.W., 1976. A laboratory model of diffusion into the convective planetary boundary layer.

Quarterly Journal of the Royal Meteorological Society 102, 427–445.

Willis, G.E., Deardorff, J.W., 1978. A laboratory study of dispersion from an elevated source within a modeled convective planetary boundary layer. Atmospheric Environment 12, 1305–1311.

Willis, G.E., Deardorff, J.W., 1981. A laboratory study of dispersion from a source in the middle of the convectively mixed layer. Atmospheric Environment 15, 109–117.

Yamada, T., Bunker, S., 1988. Development of a nested grid, second moment turbulence closure model and application to the 1982 ASCOT Brush Creek data simulation. Journal of Applied Meteorology 27, 567–578.

Yee, E., Wilson, D.J., 2000. A comparison of the detailed structure in dispersing tracer plumes measured in grid-generated turbulence with a meandering plume model incorporating internal fluctuations. Boundary-Layer Meteorology 94, 253–296.